JOURNAL OF MATERIALS SCIENCE 32 (1997) 3565–3569

# Microstructural effect on tensile and fatigue behaviour of C–Mn steel

K. HUSSAIN
*Metallurgy Division, P.O. Box, 502, Rawalpindi, Pakistan*

R. R. DE LOS RIOS
*Department of Mechanical and Process Engineering, University of Sheffield, Mappin Street, Sheffield, S1 4DU, UK*

Stress–strain behaviour in tension and in torsion was studied in ferrite–pearlite and ferrite–bainite microstructures of C–Mn steel. The fatigue tests were performed under reverse torsional loading on hour-glass shape specimens. The cyclic plasticity in torsion was found at about 37% of the monotonic yield stress in both ferrite–pearlite and ferrite–bainite microstructures. The ferrite phase in the direction of maximum shear stress was the preferable site for crack nucleation. The ferrite–bainite microstructure showed better fatigue properties than the ferrite–pearlite microstructure.

## 1. Introduction

There has been an increasing demand for economical alloys with superior mechanical properties and thus considerable effort has been directed towards improving the mechanical properties of these alloys. Progress has also been made in improving the understanding of microstructural effects on fatigue behaviour for simple alloy systems [1, 2, 3].

The fundamental material properties used in designing are monotonic and cyclic stress–strain response and the fatigue limit. The cyclic behaviour is very useful in understanding the fatigue process. Traditionally, the fatigue resistance of ferrous alloy has been based on the concept of an endurance limit. Modern approaches to fatigue design [4] emphasize fatigue as a problem in cyclic deformation. Central to these approaches for predicting component performance in service situations is a set of properties that characterizes the cyclic deformation and fracture behaviour of a material. These properties, which are related to material strength, ductility and strain hardening/softening behaviour, provide a useful quantitative basis for assessing and interpreting the influence of various microstructural features on material fatigue resistance.

The distribution and morphology of the carbide phase have been recognized to play an important role in determining the mechanical properties [5]. Gensamer [6], reported that the tensile properties depend primarily upon the mean free ferrite path irrespective of the shape of the carbide particles. He found that as the free mean path decreased the microstructure would increase in strength.

Fatigue properties of metals are quite sensitive to microstructure and a more promising approach to increasing fatigue strength appears to be the control of microstructure. In general the optimum fatigue properties can be obtained through proper heat treatment and thermomechanical treatments. A considerable effort has been made towards the relationship between the microstructure and mechanical properties of fully martensitic or bainitic steel. The mechanical properties of 0.4C–Cr–Mo–Ni steel are shown to be significantly affected by the morphology of the bainite as a second phase [7].

Bainitic microstructure can be produced in a variety of steels either as a result of a deliberate attempt to achieve a particular combination of strength and toughness or in response to welding during fabrication. In a welded component the heat-affected zone and base metal microstructure undergo similar loading, while the heat-affected zone microstructure is entirely different from the base metal microsctructure and possesses different mechanical properties. The significance of the bainite as a transformation product lies in its effect on mechanical properties.

In the present study a normalized banded ferrite–pearlite microstructure and simulated heat affected zone microstructure of a C–Mn steel were investigated. The objective of the present work was to characterize the stress–strain response and fatigue lifetime behaviour as well as the crack initiation and propagation in two different microstructures of the material.

## 2. Material and experimental technique

The material used in this investigation was a carbon–manganese steel with 0.12% C and 1.4% Mn. C–Mn steel has very good weldability characteristics and is used where a combination of high strength and outstanding weldability is required. A base metal

0022–2461  

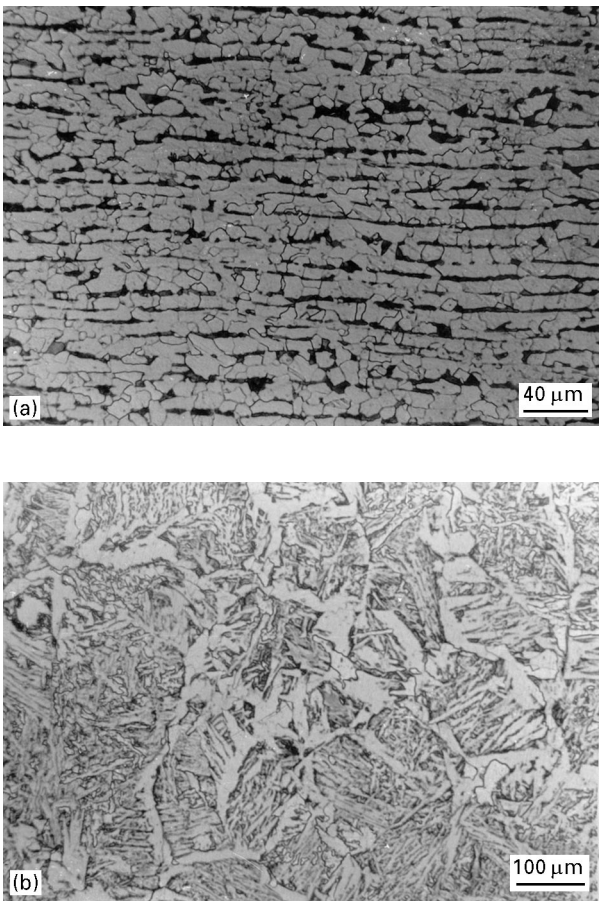


*Figure 1* Microstructure of the material: (a) banded ferrite–pearlite; (b) ferrite–bainite.

microstructure and a simulated heat-affected zone microstructure have been investigated in this study. Heat affected zone microstructure was simulated by heat treatment and is described in Ref. [8]. The ferrite phase in the base metal micrstructure (banded ferrite–pearlite) and in simulated microstructure (ferrite–bainite) was 60% and 32% and the ferrite and prior austinite grain sizes were 21 μm and 155 μm, respectively. The microstructures of the material are shown in Fig. 1.

Torsional cyclic stress–strain behaviour was studied on hour-glass shape specimens at zero mean stress. The torsional cyclic yield stress ($\Delta\tau_{cy}$) was found to be 276 MPa and 230 MPa in ferrite–bainite and ferrite–pearlite microstructures, respectively. The cyclic hardening/softening behaviour of the material is presented elsewhere [9].

Fatigue lifetime and crack initiation and propagation studies were conducted on hour-glass specimens under reverse torsional loading. Crack initiation site and its subsequent propagation was monitored by the replication of the gauge section. The replicas were taken after certain number of stress cycles. The specimen gauge section was polished and etched, prior to fatigue cycling, to reveal the microstructural interaction with crack growth.

## 3. Results and discussion

The monotonic yield stress at 0.2% strain was found to be 312 MPa and 371 MPa in ferrite–pearlite and ferrite–bainite microstructures, respectively, and is presented in Table I. The portion of the true stress–strain curve in the plastic region under monotonic loading may be described empirically by the relationship for banded ferrite–pearlite microstructure

$$\sigma = 854.53\,(\varepsilon)^{0.21} \tag{1}$$

and for ferrite–bainite microstructure

$$\sigma = 877\,(\varepsilon)^{0.17} \tag{2}$$

The hardening exponents ($n$), which reflect the ability of the material to resist further deformation are almost the same (Equations 1 and 2), in spite of a large difference of ferrite phase in both microstructures. It may be due to the difference in grain size. The effect of a large amount of ferrite phase, which is soft, is compensated by small grain size in banded ferrite–pearlite microstructure.

The determination of the cyclic yield stress is important since the development of a surface crack in smooth specimens is a plasticity-dominated process and also the minimum stress range required to induce cyclic plasticity in the material is the cyclic yield stress. The endurance limit can be associated with the point on the cyclic curve where plastic strain becomes vanishingly small. Mitchell [4] characterized the cyclic stress–strain relationship in the form of stress amplitude and plastic strain amplitude. According to Ibrahim and Miller [10], the damage accumulating in short crack propagation phase could be related to an elastic-plastic fracture mechanic (EPFM) crack growth law in the form of plastic strain amplitude.

The cyclic stress–strain response of the material, in result of multisteps tests, is shown in Fig. 2 in both microstructures. Shear stress and shear strain from the applied torque ($T$) and angular deflection ($\theta$) was calculated by using the following formulae

$$\Delta\tau = \frac{T}{2\pi r^3} \times (m+3) \tag{3}$$

for ferrite–pearlite microstructure

$$\%\Delta\gamma_t = 0.138 r\Delta\theta - 6.68\times10^{-4}\,\Delta\tau \tag{4}$$

$$\%\Delta\gamma_p = 0.138 r\Delta\theta - 1.92\times10^{-3}\,\Delta\tau \tag{5}$$

TABLE I Mechanical properties of the material in different microstructures

| Microstructure | 0.2% $\sigma_{ys}$ (MPa) | UTS (MPa) | Elongation (%) | Area reduction (%) | $\sigma_f$ (MPa) | $\varepsilon_f$ | $\Delta\tau_{cy}$ (MPa) | $\tau_{cy}/\sigma_{ys}$ | $\Delta\tau_{FL}$ (MPa) |
|---|---|---|---|---|---|---|---|---|---|
| Ferrite–pearlite | 312 | 475 | 30.22 | 76.7 | 1228 | 1.45 | 2.30 | 0.368 | 245 |
| Ferrite–bainite | 371 | 542 | 33.17 | 76.45 | 1453 | 1.44 | 276 | 0.372 | 290 |

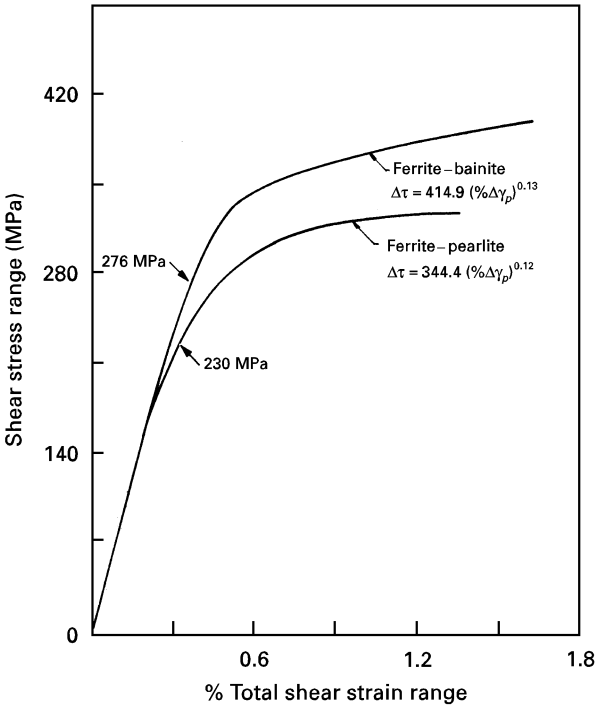


*Figure 2* Cyclic stress–strain curves of both microstructures.

for ferrite–bainite microstructure

$$\%\Delta\gamma_t = 0.133r\Delta\theta - 5.18 \times 10^{-4}\,\Delta\tau \qquad (6)$$

$$\%\Delta\gamma_p = 0.133r\Delta\theta - 1.76 \times 10^{-3}\,\Delta\tau \qquad (7)$$

$\Delta T$, $\Delta\theta$, $r$, $\Delta\tau$, $\Delta\gamma_t$, $\Delta\gamma_p$ and $m$ are torque range in N m, range of angular deflection in degrees, half of the minimum diameter of the specimen, range of shear stress, range of total shear strain, range of plastic shear strain and the slope of the $\Delta T$ versus $\Delta\theta$ curve, respectively. For the derivation of the above formulae see Ref. [11].

The crack initiation and early growth was found in the ferrite region. Cracks initiated below the fatigue limit grow only until the first barrier where they arrest, unless the stress level is increased. During the present study cracks were found to initiate at a stress level of 285 MPa, just below the fatigue limit in ferrite–bainite microstructure. Fig. 3 shows micrographs taken from replicas at different stages during the test, a crack initiated and growing in ferrite colony was stopped by a cementite plate at the end of the ferrite grain. After a large number of cycles the crack was not able to overcome the grain boundary barrier and became a non-propagating crack.

At a stress level higher than the fatigue limit, the cracks were arrested for short periods at pearlite phase in ferrite–pearlite microstructure and at cementite plate/grain boundary in ferrite–bainite microstructure, as shown in Figs 4 and 5, respectively. In the figures the arrows show the arrest point while the crack is still growing in the weaker region from the other end. In ferrite–bainite microstructure, the barrier (shown by arrow in Fig. 5b) was broken after about 400 000 cycles, as shown in Fig. 5c.

The results of the lifetime tests at zero mean stress are shown in Figs 6–8. The number of cycles to failure

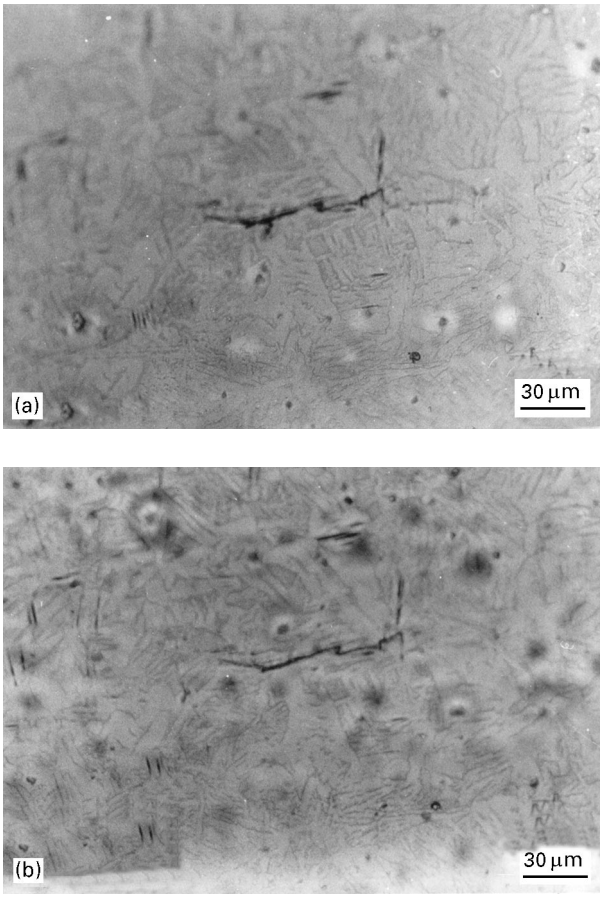


*Figure 3* Non-propagating crack in ferrite–bainite microstructure (photo from plastic replica). (a) $N = 3.7 \times 10^6$; (b) $N = 10.2 \times 10^6$.

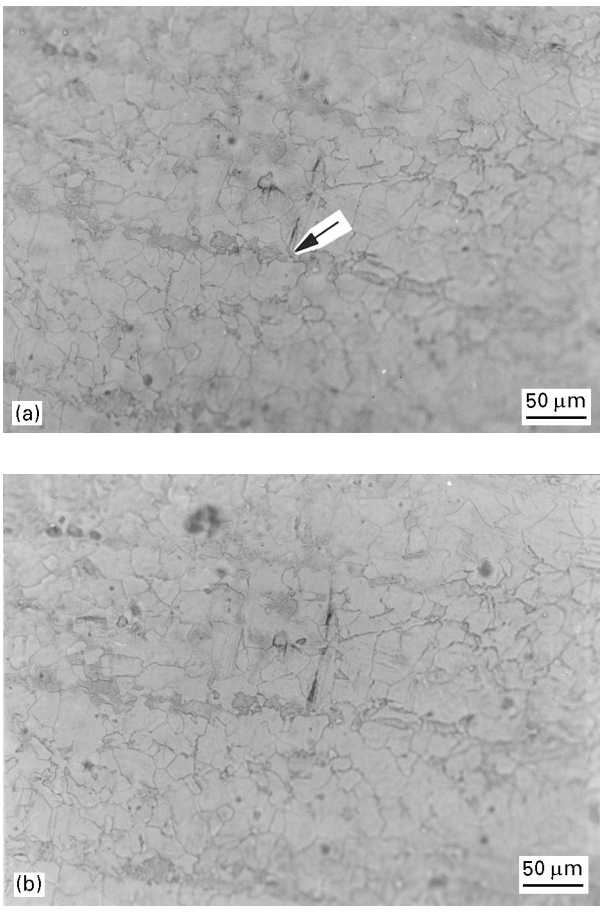


*Figure 4* Crack initiation and barrier (arrow) in ferrite–pearlite microstructure (photo from plastic replica). (a) $N = 10\,000$; (b) $N = 92\,000$; (c) $N = 500\,000$.

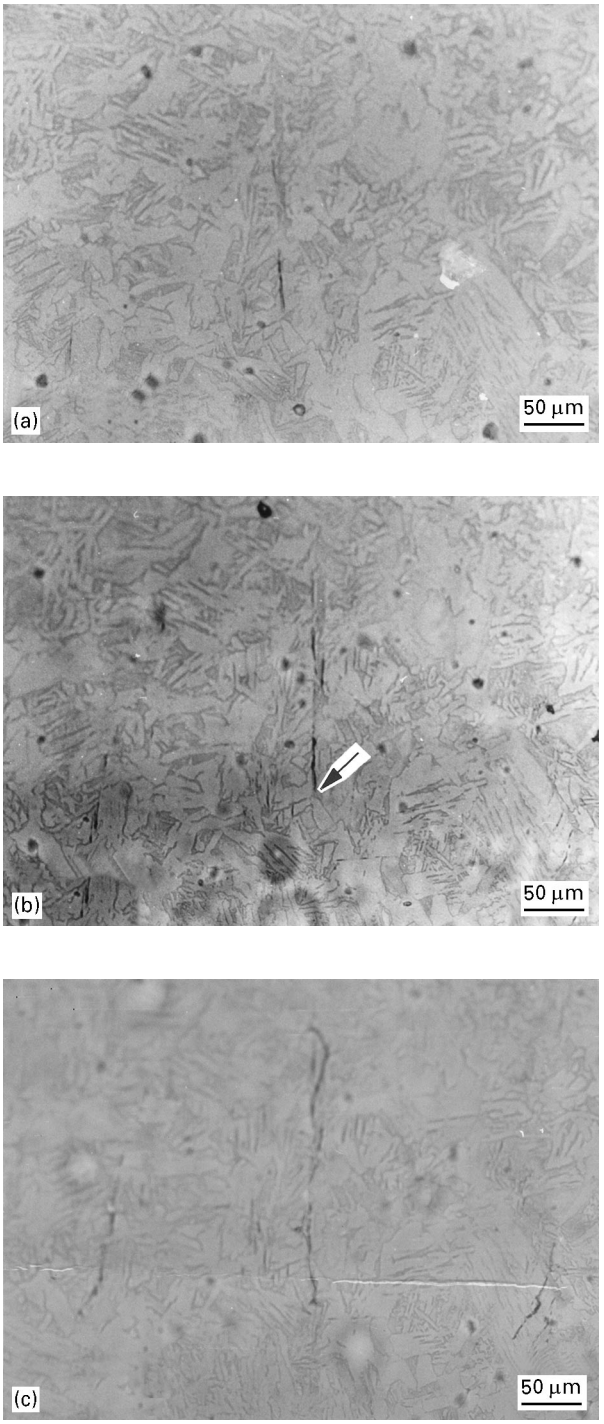


*Figure 5* Crack initiation and barrier (arrow) in ferrite–bainite microstructure (photo from plastic replica). (a) $N = 10\,000$; (b) $N = 92\,000$; (c) $N = 500\,000$.

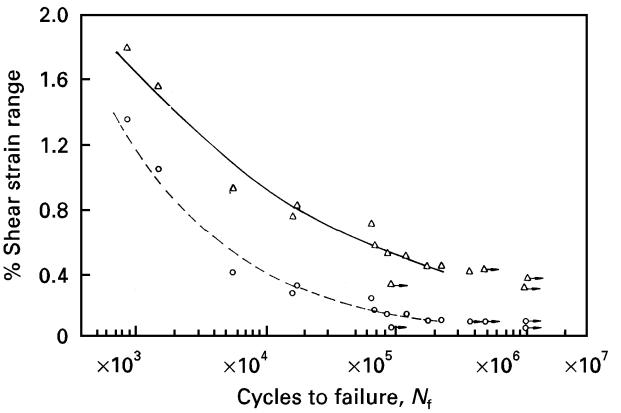


*Figure 6* Shear strain versus cycles to failure in ferrite–pearlite microstructure. (△) % $\Delta\gamma_t$; (○) % $\Delta\gamma_p$; (→) unfailed; (——), (- - - -) best fit equations. (—) % $\Delta\gamma_t (N_f)^{0.25} = 16.6$; (– – –) % $\Delta\gamma_p (N_f)^{0.46} = 78.8$.

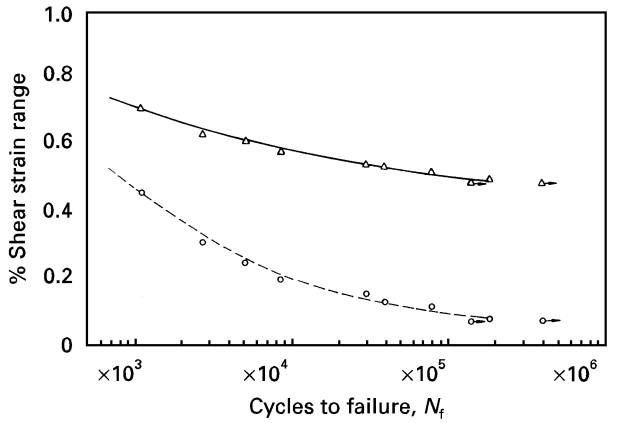


*Figure 7* Shear strain versus cycles to failure in ferrite–bainite microstructure. See Fig. 6 for key. (—) % $\Delta\gamma_t (N_f)^{0.07} = 1.3$; (- - - -) % $\Delta\gamma_p (N_f)^{0.37} = 10.8$. (△) % $\Delta\gamma_t$; (○) % $\Delta\gamma_p$; (→) unfailed; (——), (- - - -) best fit equations.

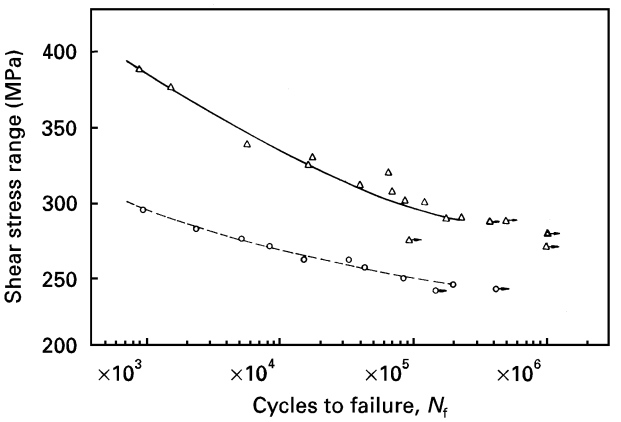


*Figure 8* Shear stress versus cycles to failure in ferrite–pearlite (○) and ferrite–bainite (△) microstructures. (△ →) unfailed; (○ →) unfailed; (——) $\Delta\tau (N_f)^{0.06} = 735.74$; (——), (- - - -) best fit equations. (– – –) $\Delta\tau (N_f)^{0.04} = 448.82$.

were recorded at 5% decay in applied torque range. The shear stress and shear strain were calculated by using Equations 3–7. The best fit line for the Coffin [12], Manson [13] and Basquin [14]-type relationships are presented in Figs 6, 7 and 8, together with experimental data.

The fatigue limits obtained under torsional loading ($\Delta\tau_{FL}$), have the values of 290 MPa and 245 MPa, which are slightly higher than the cyclic yield stresses in torsion ($\Delta\tau_{cy}$), of 276 MPa and 230 MPa for ferrite–bainite and ferrite–pearlite microstructures, respectively. It indicates that cyclic plasticity is expected to develop below the fatigue limit which supports the argument that fatigue crack initiation occurs at stress below the fatigue limit. Furthermore, this limit can be

more accurately defined as the stress below which crack can not propagate [15].

## 4. Summary

The cyclic to monotonic yield stress ratio ($\tau_{cy}/\sigma_{ys}$) were 0.368 and 0.372 which means that the plastic deformation under torsional loading will occur at $\approx 37\%$ of the monotonic yield stress in ferrite–bainite and ferrite–pearlite microstructures. The fatigue limit ($\tau_{FL}$) in both microstructures was slightly higher than the cyclic yield stress which indicates that the cyclic plasticity develops below the fatigue limit which may initiate the non-propagating cracks as it was observed in ferrite–bainite microstructure. The crack initiation and early growth was found in ferrite regions in both microstructures.


## Acknowledgements

The authors are thankful to the Government of Pakistan for a research scholarship for K. Hussain, Alcan Internationals for SIRIUS assistant directorship of research for E.R. de los Rios and Health and Safety Executive Sheffield for financial support.


## References


1. C. E. FELTNER and P. BEARDMORE, ASTM/STP 467, 1970, p. 77.
2. J. C. GROSSKREUTZ, ASTM/STP 495, 1971, p. 5.
3. C. LAIRD, "Alloy microstructural design", (Academic Press, New York, 1976) p. 175.
4. M. R. MITCHELL, "Fatigue and Microstructure" (ASM, Metals Park, OH, 1979).
5. F. BORIK and R. D. CHAPMAN, *Trans. Am. Soc. Met.* **53** (1961) 447.
6. M. GENSAMER, E. PEARSALL, W. S. PELLINI and J. R. LOW, *ibid.* **30** (1942) 983.
7. Y. TOMITA, *Mater. Sci. Technol.* **7** (1991) 299.
8. K. HUSSAIN, E. R. DE LOS RIOS and A. NAVARRO, *Engng. Fract. Mech.* **44** (1993) 425.
9. K. HUSSAIN and E. R. DE LOS RIOS, *Scripta Metall. Mater.* **28** (1993) 757.
10. M. F. F. IBRAHIM and K. J. MILLER, *Fatigue Engng. Mater. Struct.* **2** (1980) 351.
11. K. HUSSAIN, Ph.D. Thesis, Sheffield University, UK, 1990.
12. L. F. COFFIN, *Trans. ASME* **76** (1954) 931.
13. S. S. MANSON, *NACA, Research Memo TN*. (1954) 2933.
14. H. O. BASQUIN, *Proc. Amer. Soc. Testing Mater.* **10** (1910) 625.
15. K. J. MILLER, *Fatigue Fract. Engng. Mater. Struct.* **10** (1987) 93.



*Received 22 September 1995*
*and accepted 20 January 1997*